

Structure and Regulation of the CDK5-p25^{nck5a} Complex

Cataldo Tarricone,^{1,5} Rani Dhavan,^{2,5}
Junmin Peng,² Liliana B. Areces,¹
Li-Huei Tsai,^{2,3,4} and Andrea Musacchio^{1,4}

¹Structural Biology Unit
Department of Experimental Oncology
European Institute of Oncology
Via Ripamonti 435
I-20141 Milan
Italy

²Department of Pathology and

³Howard Hughes Medical Institute
Harvard Medical School
200 Longwood Avenue
Boston, Massachusetts 02115

Summary

CDK5 plays an indispensable role in the central nervous system, and its deregulation is involved in neurodegeneration. We report the crystal structure of a complex between CDK5 and p25, a fragment of the p35 activator. Despite its partial structural similarity with the cyclins, p25 displays an unprecedented mechanism for the regulation of a cyclin-dependent kinase. p25 tethers the unphosphorylated T loop of CDK5 in the active conformation. Residue Ser159, equivalent to Thr160 on CDK2, contributes to the specificity of the CDK5-p35 interaction. Its substitution with threonine prevents p35 binding, while the presence of alanine affects neither binding nor kinase activity. Finally, we provide evidence that the CDK5-p25 complex employs a distinct mechanism from the phospho-CDK2-cyclin A complex to establish substrate specificity.

Introduction

Cyclin-dependent kinases (CDKs) constitute a family of serine/threonine kinases whose activity is regulated by the interaction with proteins known as cyclins (Morgan, 1995). Although most CDKs have been implicated in the regulation of the cell division cycle, emerging evidence indicates that certain members of this family are involved in other processes. An important example is represented by CDK5, whose function is critical during neuronal development (Smith et al., 2001). The spatial and temporal pattern of CDK5 activation matches that of its activators, p35 and p39, which are primarily expressed in postmitotic neurons of the central nervous system (CNS). Targeted disruption of the mouse *CDK5* locus results in lethality around birth, with severe defects in the lamination of the cerebral cortex, hippocampus, and cerebellum (Ohshima et al., 1996). Disruption of the *p35* locus results in a milder phenotype, with inverted lamination of neurons in the cortex, defects in fasciculation

of axon fibers, and sporadic seizures in the adult mice (Chae et al., 1997; Kwon and Tsai, 1998). The *p35/p39* compound null mice display a phenotype indistinguishable from that of CDK5-deficient mice, indicating that p35 and p39 are necessary and sufficient for CDK5 function during neurodevelopment (Ko et al., 2001). Together, these observations point to an essential role of CDK5 in the migration and positioning of neurons during CNS development.

CDK5 substrates include the neuron-specific cytoskeletal proteins Neurofilament and Tau, the LIS1- and Dynein-associated protein Nudel, the synaptic protein Synapsin 1, and the Munc18/Syntaxin1A complex (Baumann et al., 1993; Fletcher et al., 1999; Hisanaga et al., 1993; Ishiguro et al., 1992; Lew et al., 1992; Matsubara et al., 1996; Niethammer et al., 2000; Paudel et al., 1993; Shuang et al., 1998). CDK5 has also been shown to phosphorylate proteins involved in functions of the mature brain. CDK5 phosphorylates DARPP32, a neuronal striatum-specific protein regulating dopamine signaling, rendering it an inhibitor of PKA (Bibb et al., 1999). Phosphorylation of DARPP32 by CDK5 was further shown to dampen the effect of chronic cocaine treatment, indicating a possible regulatory role of CDK5 in drug addiction (Bibb et al., 2001).

Deregulation of CDK5 activity upon conversion of p35 to p25 has been implicated in neurodegenerative diseases. p25 is a 208 residue C-terminal proteolytic product of p35. The accumulation of p25 in human brain tissues correlates with Alzheimer's disease affection (Patrick et al., 1999). Conversion of p35 to p25 can be induced by a variety of neurotoxic conditions including ischemia, excitotoxicity, and β amyloid peptide (Lee et al., 2000). The cysteine protease calpain is responsible for the proteolytic processing of p35 to p25 under these conditions (Kusakawa et al., 2000; Lee et al., 2000; Nath et al., 2000). Despite the fact that both p35 and p25 efficiently activate CDK5, p25 displays distinct properties from p35. First, p35 is a very unstable protein with a half-life of 20 to 30 min (Patrick et al., 1998), while p25 displays a substantially longer half-life. In addition, p35 localizes to cellular membranes by virtue of an N-terminal myristoylation motif (Patrick et al., 1999). In neurons, p35 is present throughout the entire cell including the tips of processes. p25 lacks the myristoylation site and is concentrated in the cell body and nucleus in neurons. These properties of p25 lead to deregulation of CDK5 kinase activity in vivo, which is associated with tau hyperphosphorylation, cytoskeletal disruptions, and apoptotic death of neurons (Patrick et al., 1999). Consistently, transgenic expression of p25 results in tau and neurofilament hyperphosphorylation and in cytoskeletal abnormalities (Ahlijanian et al., 2000). Together, these observations suggest that calpain-mediated cleavage of p35 to p25 may play a role in the pathogenesis of Alzheimer's disease. An elevated level of p25 has also been demonstrated in the mouse model of amyotrophic lateral sclerosis (Nguyen et al., 2001). It is thus conceivable that CDK5-p25 is a general factor involved in a broad spectrum of neurodegenerative diseases.

⁴Correspondence: amusacch@ieo.it (A.M.), li-huei_tsai@hms.harvard.edu (L.-H.T.)

⁵These authors contributed equally to this work.

Similar to other CDKs, active CDK5 is a proline-directed kinase that phosphorylates *in vitro* the amino acid sequence (S/T)PX(K/H/R) (where S or T are the phosphorylatable serine or threonine, X is any amino acid, and P is the proline residue in the +1 position that explains the definition of proline-directed kinase), and sites conforming to this consensus sequence are present in CDK5 substrates such as Neurofilament, Synapsin I, and Munc18 (reviewed in Smith et al., 2001). General principles on the structural bases of activation and substrate recognition by CDKs have been derived from crystallographic analyses of apo-CDK2 (inactive), CDK2-cyclin A (partially active), phospho-CDK2-cyclin A (maximally active), and a complex of the latter with a substrate peptide containing the sequence SPRK (Brown et al., 1999; De Bondt et al., 1993; Jeffrey et al., 1995; Russo et al., 1996). These studies clarified that cyclin A promotes the repositioning of the CDK2 PSTAIRE helix (fostering the essential interaction between Glu52 and Lys33) and a rearrangement of the activation segment (or T loop) that partially relieves the steric blockade to the active site observed in apo-CDK2 (Jeffrey et al., 1995). Maximal activation of CDK2 requires the phosphorylation by the CDK-activating kinase (CAK) of a threonine residue (Thr160 in CDK2) in the CDK2 activation segment. This step stabilizes a stretched conformation of the T loop, which is ideally suited to recognize substrates containing a proline residue in the +1 position (Brown et al., 1999; Russo et al., 1996). A very similar conformation is observed in the dually phosphorylated and active form of another proline-directed kinase, ERK2, further emphasizing the relevance of T loop conformation for the specificity of substrate recognition (Canagarajah et al., 1997). The structural studies also clarified that the preference of cyclin A-phospho-CDK2 for positively charged residues at position +3 relative to the phosphorylatable Ser/Thr originates from a direct interaction of the phosphate group of Thr160 with the positively charged side chain of the substrate (Brown et al., 1999). This observation explained biochemical experiments showing that cyclin A-phospho-CDK2 has a strong preference for substrates containing the sequence SPRK relative to SPRA, while the unphosphorylated form (which is roughly 100-fold less active than the phosphorylated form) phosphorylates these peptides with similar efficiency (Solomon and Kaldis, 1999).

This dual mechanism of CDK activation—cyclin binding and activation loop phosphorylation—has general validity for the members of the CDK family. Evidence is accumulating, however, that CDK5 may be subject to a different regulatory strategy. The p35 and p39 CDK5 activators are homologous proteins that do not share detectable sequence similarity with the cyclins. p35 and p39 bind CDK5 with exquisite selectivity and do not appreciably bind to or activate other members of the CDK family (Poon et al., 1997). Conversely, although CDK5 interacts with cyclins such as cyclin D and cyclin E, the resulting complexes are not endowed with catalytic activity, and their precise function remains obscure (Miyajima et al., 1995; Xiong et al., 1992). A further distinctive feature of CDK5 activation is that T loop phosphorylation is not required to activate CDK5-p35, and despite the presence of a phosphorylatable residue (Ser159) at a position equivalent to Thr160 of CDK2,

CDK5 is not phosphorylated by CAK *in vitro* (Poon et al., 1997; Qi et al., 1995). In view of the role played by T loop phosphorylation in CDK2 activation and substrate recognition, it is expected that p35 provides a phosphorylation-independent mechanism to tether the CDK5 T loop in an active conformation similar to those displayed by active CDK2 and ERK2. Furthermore, in the absence of T loop phosphorylation, an alternative mechanism must be present to allow the preferential recognition by CDK5 of positively charged residues at the +3 position.

The crystal structure of the CDK5-p25 protein complex provides an insight into the mechanisms that render the phosphorylation of the CDK5 activation loop superfluous for the activation of this kinase. We also present biochemical evidence that the CDK5 T loop plays a critical role in determining the selectivity of the interaction with p35. Finally, we reveal an involvement of the regulatory subunit in the recognition of positively charged substrates of the CDK5 kinase.

Results and Discussion

Structure Determination

The human p25 and CDK5 proteins were coexpressed in insect cells using a single Baculovirus vector. In order to avoid apparent toxicity from unregulated CDK5 activity, residue Asp145, located in the conserved Asp-Phe-Gly motif, was mutated to asparagine to produce an inactive kinase. The full-length CDK5 sequence was fused in frame to a C-terminal hexahistidine tag, and the protein complex was purified by immobilized metal affinity chromatography and other conventional chromatographic techniques (see Experimental Procedures). The complex crystallized in space group C2, with two p25-CDK5 complexes in the asymmetric unit (Table 1). The structure was determined at a resolution of 2.65 Å using a combination of Molecular Replacement and density modification techniques (see Experimental Procedures). The electron density maps displayed good density for CDK5 and for residues 147 to 293 of p25. The N-terminal segment and 14 C-terminal residues of p25 were invisible in the electron density. The model has been refined to a crystallographic R factor of 24.2% and a free R factor of 28.2% for all data between 20 and 2.65 Å, with good stereochemical parameters (Table 1).

The p25 Globular Domain

A ribbon diagram of the p25-CDK5 complex is shown in Figure 1. CDK5 is structurally very similar to CDK2, as expected from a sequence identity of 60% between these kinases. Residues 147 to 293 of p25 fold into a globular domain (p25^{GD}) whose position relative to the kinase moiety is closely reminiscent of that occupied by cyclin A when bound to CDK2 (Jeffrey et al., 1995). There are eight α helices in the p25^{GD} (Figure 1). We define the first helix as the N-terminal helix (α NT), while the remaining seven helices are named α 1 to α 7 (Figure 2A). Helices α 1 to α 5 adopt a topology similar to the cyclin-box fold (CBF), the structural motif present in the cyclins (Gibson et al., 1994; Noble et al., 1997). The uncertain phylogenetic origin of p25 and its structural differences with bona fide members of the CBF family prompted us to adopt the definition of CBF-like motif

Table 1. Structure Determination of the CDK5-p25 Complex

Data Statistics			
Data Set	C2	C2221 (I)	C2221 (II)
Unit cell dimensions	a = 149.0 b = 89.8 c = 82.6 β = 93.0	a = 89.5 b = 144.6 c = 82.0	a = 87.8 b = 141.8 c = 81.0
Resolution (Å)	20–2.65	15–3.20	12–3.55
Observations/unique reflections	67318/32449	22615/9160	19436/6207
Completeness (last shell)(%)	93.9 (78.5)	97.2 (93.2)	97.8 (91.6)
R _{sym} ^a (last shell)(%)	4.3 (23.3)	6.1 (43.2)	7.7 (15.9)
I/σI (last shell)	16.3 (3.6)	13.1 (1.5)	13.0 (4.1)
Refinement Statistics			
Data Set	C2		
Resolution (Å)	20–2.65		
Protein atoms	6982		
Reflections (working set/test set)	28718/1506		
R _{cryst} ^b (%)	24.2		
R _{free} ^c (%) (of data)	28.4 (5)		
R.m.s. bonds (Å)	0.021		
R.m.s. angles (°)	2.3		

$$^a R_{\text{sym}} = \frac{\sum_{hkl} \sum_i |I_i(hkl) - \overline{I(hkl)}|}{\sum_{hkl} \sum_i I_i(hkl)}$$

$$^b R_{\text{cryst}} = \frac{\sum_{hkl} |F_{\text{obs}} - kF_{\text{calc}}|}{\sum_{hkl} |F_{\text{obs}}|}$$

^c R_{free} is equivalent to R_{cryst} but is calculated using a disjoint set of reflections excluded from the refinement stages.

(CBFL), rather than CBF, whose use will be limited to cyclins and related proteins.

Ribbon diagrams of the p25^{GD} and of cyclin A (residues 175–432 of human cyclin A) are shown in Figures 2A and 2B, respectively. In contrast to cyclin A, which contains tandem copies of the CBF (Brown et al., 1995; Gibson et al., 1994; Jeffrey et al., 1995), there is a single CBFL region in p25. This is not a distinguishing feature of p25, however, as a survey of the SMART database shows that there are several instances of proteins containing a single copy of the bona fide CBF domain (Schultz et al., 2000). Cables, a recently identified CDK5 ligand (Matsuoka et al., 2000; Zukerberg et al., 2000), contains a segment (residues 430–550 of the mouse sequence) whose structural similarity with the CBF is strongly supported by threading analysis (Jones, 1999). An alignment of the Cables CBF to the first CBF of cyclin A is shown in Figure 2C. Single CBFs are also found in the Pcl-type cyclins and Pho80, activators of the functional homolog of CDK5 in budding yeast, Pho85 (Moffat et al., 2000).

Most contacts of cyclin A with CDK2 map to the N-terminal helical segment (αNT, gray) and to the first CBF motif (orange), and our comparison with p25 can be limited to this region. The progression of secondary structure in the p25^{GD} is similar to that of cyclin A, with an N-terminal helix (gray) followed by the CBFL region (helices α1–α5, in yellow). The CBFL is followed by two additional helices (α6–α7 in red) that pack against the core of the domain to bring the N- and C-terminal regions in close proximity (Figure 2A). Although the p25^{GD} represents only a fragment of the p35 and p39 activators, we feel that other globular domains are unlikely to be present in these proteins. This is supported by the fact

that the conservation of structurally or functionally important residues in p35 and p39 is precisely limited to the p25^{GD} (Figure 2C). In addition, the p35 and p39 segments neighboring the p25^{GD} region do not appear to contain enough apolar residues to support the formation of a stable hydrophobic core (Figure 2C), and several proline and glycine residues may further counteract high order structuring. Consistent with this view, the N-terminal region of p25 (residues 99–146) is invisible in the electron density maps and is readily removed from the p25-CDK5 complex by limited proteolysis (data not shown). Thus, we suggest that p35 and p39 share a similar structural organization, consisting of relatively large and unstructured N-terminal regions and a C-terminal globular domain with the same topology and functional properties of the p25^{GD} revealed by our crystal structure. The N-terminal segments of p35 and p39 play a role in protein localization, may regulate their stability, and may act as a docking site for CDK5 regulators.

The p25-CDK5 Interaction

The p25^{GD} and the N-terminal region of cyclin A adopt a similar position on their cognate kinases, and an equivalent surface area is buried (roughly 3400 Å²). The details of the interactions, however, are not easily amenable to a direct comparison due to the structural differences between these domains. The αNT helix may be an important determinant of these differences. In cyclin A or a γ-herpesvirus cyclin (M-cyclin), this element is extensively implicated in CDK2 binding (Card et al., 2000; Jeffrey et al., 1995), while the αNT of p25 does not interact with CDK5 (Figure 2C). The reported interaction between CDK5 and a peptide corresponding to the p25

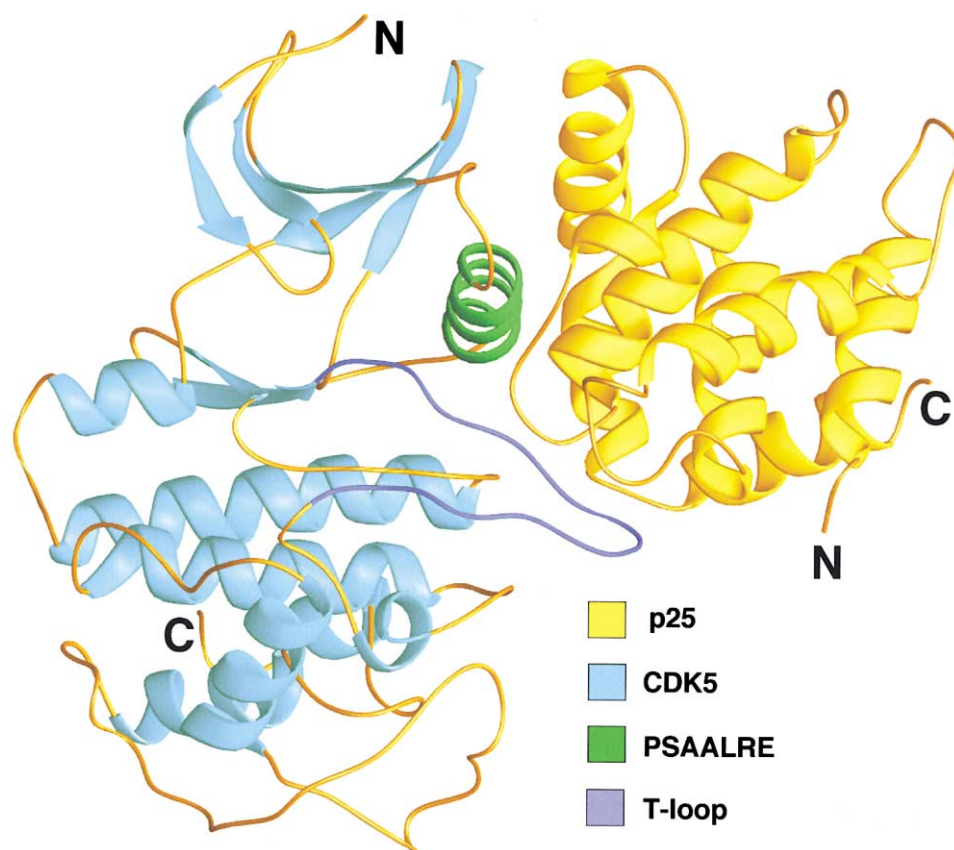


Figure 1. Structure of the CDK5-p25 Complex from the Standard Front View Ribbon Diagram of p25-CDK5

p25 (yellow) binds CDK5 (light blue) in the region of the PSSALRE helix (green) in the kinase small lobe. There are extensive contacts with the activation loop (dark blue). The position of the N and C termini is shown. Figures 1–4 and 6A were created using programs Ribbons and GRASP (Carson, 1991; Nicholls et al., 1991).

α NT helix is inconsistent with our structural data (Chin et al., 1999). In p25, α NT packs tightly against α 1, α 2, and the last portion of the α 7 helices (Figure 2). A close contact between Gly156^{p25} in the α NT helix and Pro171^{p25}, located at the beginning of α 1, displaces α 1 into a significantly different position from that observed in cyclin A (Figure 3). As a consequence of this arrangement, the α 4 and α 5 helices also adopt a different position in p25 and appear to be related to their cyclin counterparts by a concerted rotation. The structural differences explain retrospectively the difficulties in producing accurate structural alignments of p25 on cyclin A using threading methods or other approaches (Brown et al., 1995; Chou et al., 1999; Tang et al., 1997).

The overall result of these positional differences is that the α 1- α 2 and α 3- α 4 loops of p25 approach the kinase moiety, and the activation loop in particular, much more closely than the equivalent segments of cyclin A (Figure 3). This does not affect the relative position of the PSSALRE (CDK5) and PSTAIRE (CDK2) helices, which adopt an identical position in CDK5-p25 and in cyclin A-phospho-CDK2 (Figure 3). Although a structure of apo-CDK5 is not available, we assume that p25 triggers a similar conformational rearrangement of the PSSALRE helix, and, more generally, of the CDK5 small lobe, to that observed upon cyclin A binding to apo-CDK2.

More significant to understanding the structural bases of CDK5 activation are the extensive contacts made by p25 with the activation loop of CDK5, a feature that is not observed in CDK-cyclin complexes (Figure 4). A surface representation of the bottom surface of the p25^{GD} (Figure 4A) shows the presence of a ridge, rather hydrophobic in character, formed by residues located in the last portion of the α 3 and α 6 helices, and by the loops that follow these helices. Residues 148–153 of CDK5, located in the activation loop, are accommodated into this ridge. The side chain of Ile153^{CDK5}, at the bending tip of the activation loop, fits snugly into a pocket formed by the side chains of A199^{p25} (α 1- α 2 loop), Met237^{p25} (α 3 helix), Ile275^{p25}, Ala277^{p25}, Pro279^{p25}, and Phe282^{p25} (α 6- α 7 loop). Thus, the interaction of p25^{GD} with CDK5 involves residues located outside the CBFL region, in particular in the α 6 helix and the α 6- α 7 loop (Figure 2C). The interaction is completed by the α 3- α 4 loop, which pushes against the CDK5 activation loop, in particular through the side chains of Asn239^{p25} and Ile241^{p25}. The p25 residues participating in CDK5 binding are almost completely invariant in p35 and p39 across species (Figure 2C).

Snapshot of an Active Kinase Conformation

The overall effect of the interactions described above is that the activation loop of CDK5 is tethered in an

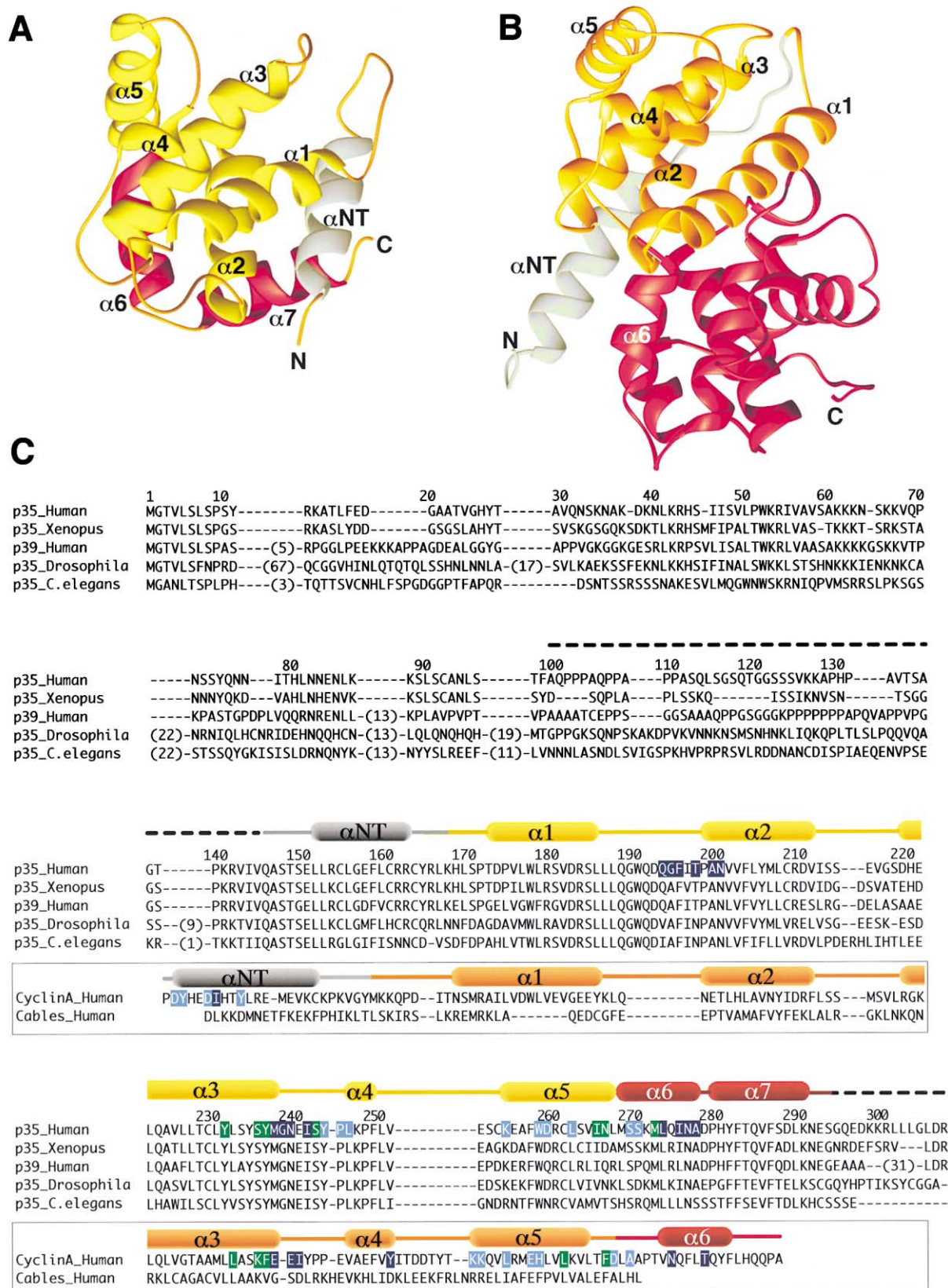


Figure 2. Comparison of p25 and Cyclin A

(A) Ribbon diagram of the p25⁶⁰ with a view identical to that adopted in Figure 1. The p25⁶⁰ includes the αNT helix (gray), the CBFL (yellow; helices α1 to α5), and the α6 and α7 helices (red).

extended conformation that closely resembles those observed in the mono- and dually phosphorylated and fully active forms of CDK2 and ERK2, respectively (Figure 4B). Structure determination of the phospho-CDK2-cyclin A complex with a peptide containing the SPRK sequence by Brown and collaborators (1999) showed that the interaction of CDK2 with proline in the +1 position of the substrate requires the repositioning of the carbonyl group of Val163, which is triggered by the phosphorylation of Thr160. This creates a binding pocket for the proline side chain and disfavors the binding of substrates with residues other than proline, which would remain with an uncompensated hydrogen bond for the main chain NH group of the +1 residue (Brown et al., 1999). Precisely the same strategy has been adopted by active ERK2, another proline-directed kinase (Canagarajah et al., 1997). In CDK2, the repositioning of the carbonyl of Val163 is triggered by Val164, which adopts a left-handed conformation ($\phi = 72.5^\circ$, $\psi = 130.8^\circ$) that is stabilized by a network of hydrogen bonds (Brown et al., 1999; Russo et al., 1996). Phosphorylation also leads to the loss of a short helical turn in the region of Thr160, resulting in the elongation of the CDK2 activation loop.

Figure 4B shows the excellent superposition of the activation loops in the CDK5-p25 and phospho-CDK2-cyclin A complexes. After superposition of the respective kinase moieties, the C α atom of Ser159^{CDK5} is 5.1 Å away from the C α atom of unphosphorylated Thr160^{CDK2} but only 1.3 Å away from the C α atom of phospho-Thr160^{CDK2}. More significantly, the main chain dihedral angles for the CDK5 residue Val163 ($\phi = 71.7^\circ$, $\psi = 135.9^\circ$) are very similar to those of the equivalent CDK2 and ERK2 residues Val164 and Ala187, respectively. The identification of this conformation in CDK5-p25 shows that our model represents the active conformation of CDK5. Our observation is unlikely to be a consequence of phase bias, as the model of unphosphorylated CDK2 (PDB ID code 1fin) was used in molecular replacement (Jeffrey et al., 1995), and model rebuilding was required to account for the observed electron density of the activation loop (see Experimental Procedures). We assume that the Asp to Asn substitution at position 145 is unlikely to affect the conformation of the activation loop, because the conformation of the main chain around this residue in p25-CDK5, CDK2-cyclin A, and phospho-CDK2-cyclin A is essentially identical.

Thus, an important difference between the activation mechanism of CDK5 and that of other proline-directed kinases, such as ERK2 and CDK2, is that the active T loop conformation of CDK5 is not stabilized by phosphorylation but by extensive interactions with the regulatory moiety. The finding that this interaction bypasses the requirement for activation loop phosphorylation is consistent with a number of observations. First, the substitution of S159^{CDK5} with alanine does not impair the

activity of a CDK5-p25 complex reconstituted from recombinant proteins (Poon et al., 1997). Furthermore, the specific activity of unphosphorylated recombinant CDK5-p35 is similar to that of the complex purified from brain extracts, and p25-CDK5 and phospho-CDK2-cyclin A have similar specific activities (Qi et al., 1995). Finally, mouse CAK does not phosphorylate human CDK5 *in vitro* under conditions that lead to the effective phosphorylation of CDK2 on Thr160 (Poon et al., 1997). Our data apparently contradict the observations of Sharma and collaborators (1999a), who found that phosphorylation of recombinant CDK5 by an activity in PC12 lysates results in increased catalytic activity, while the CDK5^{S159A} mutant did not show similar activation. A possible explanation of these results is that CDK5 undergoes stimulatory phosphorylation at sites other than Ser159 and that the mutant is insensitive to this stimulation.

Interaction of p25 with Residues of the CDK5 T Loop Might Determine Binding Specificity

The p25-CDK5 interaction is very selective, and members of the CDK family other than CDK5 are unable to bind p25 with high affinity (Poon et al., 1997). This has to be reconciled with the limited degree of sequence variation within the CDK alignment, in particular at the positions that our structure implicates in p25 binding. The extensive involvement of the CDK5 activation loop in p25 recognition led us to speculate that some level of discrimination against incorrect matches may arise from specific contacts involving this region of CDK5. The interaction of Ile153^{CDK5} with its binding pocket on p25 (Figure 4A) may contribute to the selectivity of binding. CDK4 and CDK6, which contain a bulky aromatic residue at this position (Figure 4C), are completely unable to interact with p25, whereas CDKs with smaller residues at this position display some residual binding activity (Poon et al., 1997). To determine the importance of Ile153^{CDK5} in p35 binding, we cotransfected Cos7 cells with p35 and either wild-type CDK5 (CDK5^{WT}) or mutants in which Ile153 was replaced with alanine (CDK5^{I153A}) or phenylalanine (CDK5^{I153F}). The presence of CDK5 in p35 immunoprecipitates was then examined by Western blot (Figure 5A). While CDK5^{WT} and CDK5^{I153A} were able to interact with p35 with equal affinity, association of CDK5^{I153F} with p35 was severely impaired. Ile153 is therefore critical for association with p25 and could contribute to the selectivity of the p35-CDK5 interaction.

Another distinguishing feature of the CDK5 T loop is the presence of serine rather than threonine at position 159 (Figure 4C). The side chain atoms of Ser159^{CDK5} are in van der Waals contact with the side chains of Asn239^{p25} and Ile241^{p25} in the $\alpha 3$ - $\alpha 4$ loop (Figure 4A), and the addition of a phosphate group to Ser159 would generate a steric clash between the interacting surfaces.

(B) The N-terminal CBF of cyclin A (orange) is embedded in a different structural context, between the α NT helix, which occupies a different position relative to p25, and a C-terminal CBF (red).

(C) Sequence alignment of p35 and p39 and comparison with cyclin A and cables. Numbering refers to human p35. The secondary structure is shown with the same coloring scheme used in (A) and (B). Dashed segments represent regions that were not visible in the electron density. Positions with at least one atom within 3.8 Å of the CDK moiety are highlighted with the color of the contacting kinase element (green, PSSALRE helix; dark blue, T loop; light blue, other). The alignment in the $\alpha 1$ - $\alpha 5$ fragment was suggested by the superposition of cyclin A and the CBF of p25.

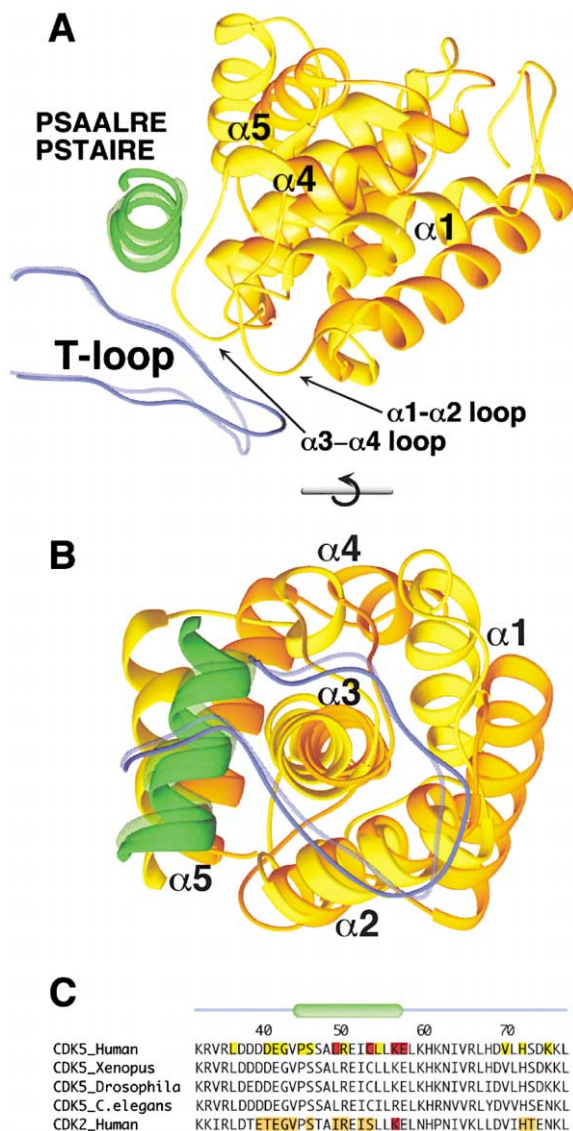


Figure 3. The p25 and Cyclin A after Superposition of the Respective Kinase Moieties

(A) The CBFL (yellow) and the N-terminal CBF of cyclin A (orange) are compared after superimposing the respective kinases. Only the PSAALRE/PSTAIRE and the activation loops of CDK5 (full color) and CDK2 (half-tone) are shown. Other structural elements were removed to improve clarity. The $\alpha 3$ - $\alpha 4$ loop of p25 forms a wedge between the activation loop and the PSSALRE helix. In (B), the molecule is viewed after a rotation of 90° about a horizontal axis. The CBFL engages in a more intimate interaction with CDK5 relative to CDK2-cyclin A and has a rather different orientation. The $\alpha 2$ and $\alpha 3$ of p25 and cyclin A superimpose well, but $\alpha 1$, $\alpha 4$, and $\alpha 5$ are related by a concerted rotation about an axis roughly parallel to $\alpha 3$. (C) Sequence alignment of the PSSALRE/PSTAIRE helix of CDK5 and CDK2. The positions of the corresponding secondary structure elements are shown. Positions with at least one atom within 3.8 Å from the respective activator are highlighted using the coloring scheme adopted in (A) and (B).

In fact, even an apparently conservative substitution, such as that with threonine, may be sufficient to adversely affect binding. To test the role of Ser159 in p35 recognition, we cotransfected Cos7 cells with p35 and

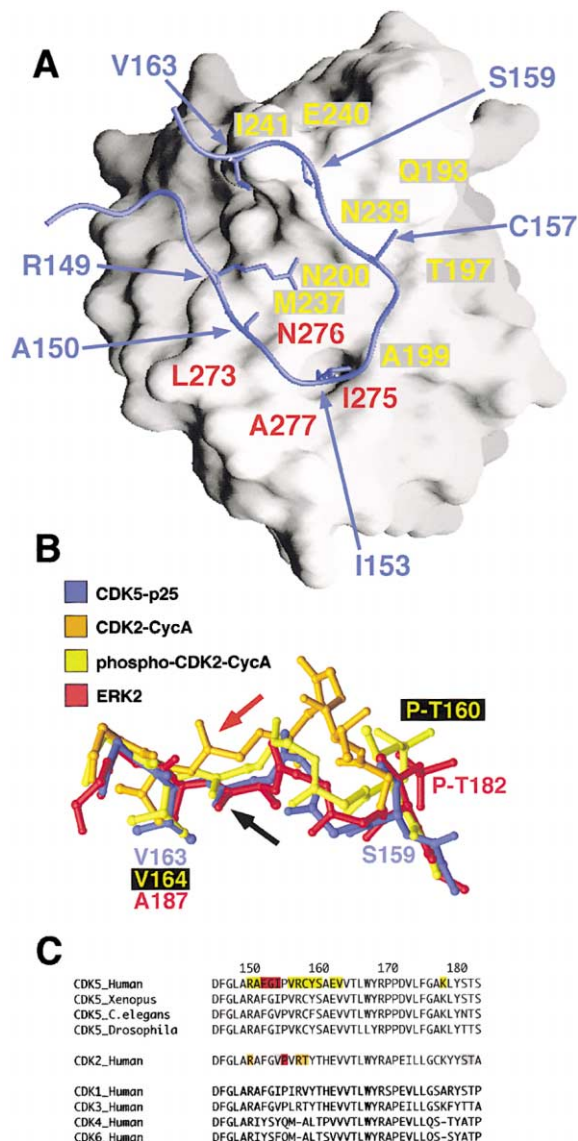


Figure 4. Comparison of Activation Loop Conformation in CDK2, CDK5, and ERK2

(A) Surface representation of p25 with the CDK5 activation loop. The view is similar to that used in Figure 3B. The position of important residues is labeled on the molecular surface (yellow for residues in the CBFL, red for residues in $\alpha 6$ - $\alpha 7$). The activation loop (dark blue) is shown together with side chains directed toward the p25 surface. Note the binding pocket occupied by the side chain of Ile153. (B) The conformation of the T loop in CDK2-cyclin A (orange), phospho-CDK2-cyclin A (yellow), phospho-ERK2 (red), and CDK5-p25 (blue). The T loop of CDK5 adopts the same conformation observed in phosphorylated CDK2 and ERK2. (C) Sequence alignment of the activation loops of several CDKs. Colored positions within the CDK5 and CDK2 sequences identify residue within 3.8 Å from the activator moiety, and the color defines particular regions of the activators, according to the scheme adopted in Figure 2.

either CDK5^{WT} or mutants in which Ser159 has been changed to alanine (CDK5^{S159A}), threonine (CDK5^{S159T}), or glutamic acid (CDK5^{S159E}). While CDK5^{WT} or CDK5^{S159A} coimmunoprecipitated with p35 with equal affinity, association of CDK5^{S159E} with p35 was severely impaired (Figure 5B). Binding of CDK5^{S159T} to p35 was also greatly

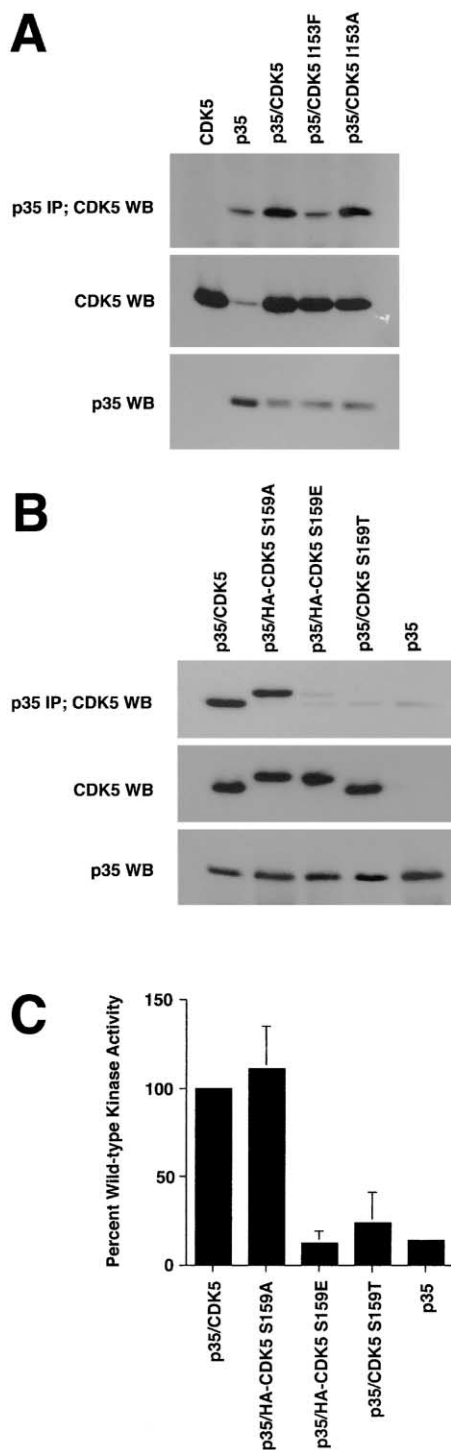


Figure 5. Ile153 and Ser159 in the T Loop of CDK5 Are Critical for p35 Binding

(A) Role of Ile153^{CDK5} in p35 binding. Cos7 cells were transfected with p35 and either no exogenous CDK5, wild-type CDK5, CDK5-I153F, or CDK5-I153A. p35 was immunoprecipitated from transfected lysates, followed by anti-CDK5 Western blot (top panel). 10 μ g of the transfected lysates was Western blotted for CDK5 (middle panel) or p35 (bottom panel).

(B) Role of Ser159^{CDK5} in p35 interaction and kinase activity. Cos7 cells were transfected with p35 and either wild-type CDK5 or HA-CDK5-S159A, HA-CDK5-S159E, CDK5-S159T, or no exogenous

diminished, but the levels of association varied somewhat from experiment to experiment, ranging from about 10% to 40% of the binding levels of the WT protein. Kinase activity of the p35 immunoprecipitates correlated with the degree of association of the CDK5 variants with p35 (Figure 5C). Our results suggest that the presence of serine rather than threonine at position 159 of CDK5 is a critical determinant of binding selectivity. Furthermore, our observation likely explains why other CDK family members that contain a threonine at the equivalent position are unable to form high-affinity complexes with p25 (Poon et al., 1997). Finally, the fact that a mutation that mimics a phosphorylated state completely inhibits p35 (and presumably p39) binding suggests that the phosphorylation of Ser159, if occurring, will negatively regulate CDK5 activity.

p25 Contributes to Substrate Specificity

Our results show that p25 triggers all conformational changes required for CDK5 activation in the absence of activation loop phosphorylation. Like other CDKs, CDK5 has a strong preference for positively charged residues in the +3 position. For CDK2-cyclin A, the phosphorylation of Thr160 is essential to encode this specificity. On the other hand, this specificity is expected to be a phosphorylation-independent property of CDK5-p25. To shed light on this issue, we generated a rough model of the interaction of CDK5-p25 with a peptide substrate. We did this by superimposing the atomic coordinates of CDK5 and CDK2 as they occur in CDK5-p25 and in the complex of phospho-CDK2-cyclin A with a peptide containing the SPRK sequence (Brown et al., 1999). This analysis showed that the α 3- α 4 loop of p25 is likely to play a role in substrate recognition, in view of its proximity to the CDK5 substrate binding site (Figure 6A). In particular, we noticed that Glu240 in this loop appears to be in a favorable position to interact with a positively charged residue in the +3 position of the substrate. To test this hypothesis, we generated recombinant variants of p20 (a shorter version of p25 containing only the p25^{GD}) in which Glu240 was mutated into glutamine (p20^{E240Q}) or alanine (p20^{E240A}). Both mutants bound CDK5 with high affinity and precipitated equal or higher amounts of CDK5 compared to the wild-type p20 protein in GST pull-down assays (Figure 6B). We regenerated recombinant CDK5 activity by mixing bacterially expressed p20 (wild-type or mutant proteins) with bacterially expressed CDK5 and then compared the ability of the CDK5-p20 complexes to phosphorylate a synthetic peptide of sequence PKTPAKAKKL (abbreviated as TPAK) (Figure 6C). The p20^{E240Q} complex has a 6.2-fold reduction in kinase activity compared to the wild-type

CDK5. p35 was immunoprecipitated from transfected lysates followed by anti-CDK5 Western blot (top panel). 10 μ g of the transfected lysates was Western blotted for CDK5 (middle panel) or p35 (bottom panel).

(C) p35 was immunoprecipitated from the transfected cell lysates described in (B), and the kinase activity associated with p35 was measured by in vitro immune-complex kinase assays using a synthetic peptide (PKTPAKAKKL) as substrate. Kinase activity is expressed as a percent of the activity of the immune complex precipitated from Cos7 cells transfected with p35 and wild-type CDK5.

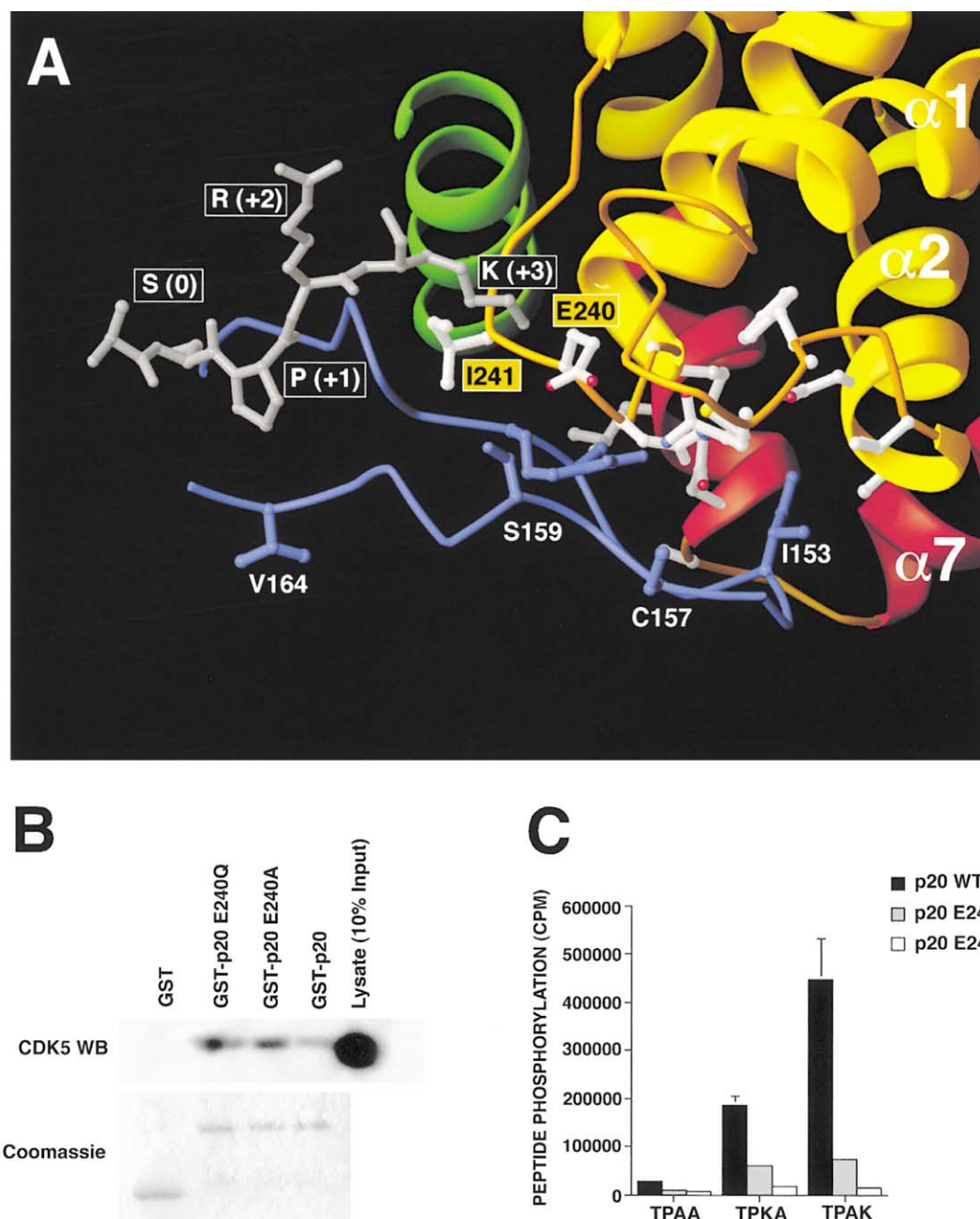


Figure 6. Role of Glu240^{p25} in Substrate Recognition

(A) A model of the SPRK peptide (Brown et al., 1999) bound to CDK5. The side chain of lysine at the +3 position may be involved in an interaction with residue Glu240 of p25.

(B) 10 μ g of GST, GST-p20, GST-p20 E240Q, or GST-p20 E240A crosslinked to Glutathione Sepharose resin was used to precipitate CDK5 from Cos7 lysates transfected with CDK5, followed by an anti-CDK5 Western blot (top panel). 5 μ g of each of the GST protein preparations used in the top panel was run on a 10% SDS-PAGE gel before crosslinking and stained with Coomassie blue to show equal levels of protein.

(C) 4 μ g of GST-CDK5 and either GST-p20, GST-p20 Glu240Q, or GST-p20 Glu240A was combined to reconstitute CDK5-p20 kinase complexes in vitro. The kinase activity of these three complexes was measured in an in vitro kinase assay using three different synthetic peptides as substrates: PKTPAKAKKL (TPAK), PKTPKAAKKL (TPKA), and PKTPAAAKKL (TPAA). Kinase activity is expressed as the amount of phosphate incorporated into the peptide substrates in counts per minute (cpm).

complex. The kinase activity of the p20^{E240A} complex was severely impaired, with a 33-fold reduction in peptide phosphorylation relative to the wild-type complex. This is in agreement with the findings of Tang et al. (1997) that p20^{E240A} has a 90% reduction in CDK5 activation

compared to wild-type p25, although the mutant protein binds CDK5 with wild-type affinity. This suggests that Glu240^{p35} is important for maximal activation of CDK5.

To investigate the potential role of this residue in substrate recognition, we compared phosphate incorpora-

tion by wild-type and mutant complexes using the TPAK peptide and two other peptides of sequence PKT PKAAKKL (TPKA) and PKTPAAKKL (TPAA) as substrates (Figure 6C). The wild-type complex preferred the TPAK peptide 2.4-fold over the TPKA peptide and 16.8-fold over the TPAA peptide. Thus, the unphosphorylated CDK5-p25 complex discriminates in favor of a positive charge in the +3 position, in agreement with previous reports (Beaudette et al., 1993; Sharma et al., 1998, 1999b; Songyang et al., 1996). The p20^{E240Q} and p20^{E240A} kinase complexes were unable to distinguish between the TPAK and TPKA peptides and phosphorylated both with identical efficiency. The mutants also displayed a 6.2- and 33-fold reduction in activity toward the TPAK peptide relative to the WT protein, but only a 2.7- and 4.8-fold reduction in mutant activity toward the TPAA peptide. These results strongly implicate Glu240^{p35} in the recognition of the basic residue in the +3 position of the substrate, indicating that p35 directly participates in substrate recognition, presumably via the creation of a negatively charged environment in the proximity of the ligand binding site. The fact that both mutants displayed residual preference for the TPAK and TPKA peptides over the TPAA peptide suggests that other CDK5 or p25 residues are probably involved in the substrate recognition process. Further structural and biochemical analyses will be required to shed light on this issue.

Conclusion

The interaction of p25 with CDK5 stabilizes an active conformation of the T loop, which is indistinguishable from those observed in phosphorylated CDK2 and ERK2. We provide evidence that Ile153 and Ser159 in the T loop of CDK5 are critical for p25 and p35 recognition and might contribute to the selectivity of the CDK5-p35 interaction. Retention of serine in all CDK5 homologs from yeast to human suggests that the presence of a phosphate acceptor at position 159 might be relevant for CDK5 regulation. We predict that phosphorylation of Ser159^{CDK5}, if occurring, would negatively regulate kinase activity. It has been shown previously that phosphorylation of Tyr15 on CDK5 by Abl is stimulatory (Zukerberg et al., 2000), while phosphorylation of Tyr15 and Thr14 by Wee1 family kinases is inhibitory for CDK1 and 2. When taken together, these observations indicate that phosphorylation and dephosphorylation events similar to those impinging on mitotic CDKs regulate CDK5 in a completely distinct fashion. We also provide structural and biochemical evidence that the CDK5-p25 complex has devised a novel and distinct mechanism for substrate recognition and specificity entailing the participation of the activator subunit. In conclusion, we reveal here the molecular mechanism for CDK5 activation by p25 and identify a number of key residues that are important for CDK5 activity and could potentially serve as regulatory sites for this kinase. This work provides important clues as to how CDK5 can be regulated in post-mitotic neurons, an area that is yet to be explored. Given the involvement of CDK5 in diseases of the nervous system, this study can also help to develop strategies to combat these diseases by manipulating CDK5 kinase activity.

Experimental Procedures

Expression and Purification

The cDNAs encoding human full-length CDK5 and residues 99–307 of human p35 (coinciding with p25) were subcloned in the pBAC4X-1 transfer vector (Novagen), and the resulting baculovirus was used for coexpression in insect cells. Insect cells were harvested by centrifugation, resuspended in lysis buffer (50 mM Tris [pH 8.0] and 200 mM NaCl), sonicated gently, and the lysates were cleared by centrifugation. CDK5-p25 was absorbed to Ni-NTA agarose (Qiagen) and eluted using lysis buffer supplemented with 250 mM imidazole. DTT and EDTA were immediately added to final concentrations of 5 mM and 2 mM, respectively. The eluted protein was dialysed against buffer A (20 mM Mes [pH 6.0], 50 mM NaCl, 5 mM DTT, and 2 mM EDTA) and further purified on an FPLC (Pharmacia) using S-sepharose HP (Amersham-Pharmacia) equilibrated with buffer A. The complex eluted in a single peak using a NaCl gradient from 100 to 300 mM. The protein was concentrated by ultrafiltration and loaded onto a Superdex 200 column (Amersham-Pharmacia) equilibrated with buffer B (25 mM [pH 8.0], 100 mM NaCl, 2 mM DTT, and 1 mM EDTA). The elution volume was consistent with a 1:1 complex devoid of further oligomerization.

Crystallization and Structure Determination

Initial crystals of CDK5-p25 were generated by vapor diffusion at 20°C using a reservoir buffer containing 20% PEG3350 and 200 mM NaI (Hampton Research, Inc.) and a protein concentration of 7 mg/ml, and improved by microseeding. Crystals were gradually transferred to cryo-buffer (10% PEG3350, 100 mM Tris [pH 7.6], 200 mM KI, 10 mM DTT, and 25% glycerol) and flash-frozen prior to data collection. X-ray diffraction data from a monoclinic crystal and two orthorhombic crystals were collected on a Mar CCD (Mar Research, Germany) at beamline BW7A at EMBL-DESY ($\lambda = 1.0079 \text{ \AA}$). Data processing was carried out with DENZO and SCALEPACK (Otwinowski, 1993). For subsequent calculations, we used the CCP4 (Collaborative Computational Project, 1994) and CNS (Brunger et al., 1998) suites. Molecular Replacement was carried out using AMoRe (CCP4). The CDK2 search model was extracted from PDB ID code 1fin, representing CDK2-cyclin A (Jeffrey et al., 1995). The two solutions in the monoclinic space group were related by perfect 2-fold noncrystallographic symmetry (NCS). The correlation coefficient and R factor after rigid body fitting were 48.0% and 48.5%, respectively, for the monoclinic crystals. Initial phases were improved by solvent flattening using DM. A solvent boundary for the p25 subunits became evident, and NCSMASK (CCP4) was used to generate a mask corresponding to a CDK5-p25 complex. The electron density was then improved by multicrystal averaging as implemented in the DMMULTI program (CCP4), using the two complexes present in the monoclinic form and including the two orthorhombic forms. The new maps showed clear density for p25, and a polyaniline model was built with program "O" (Jones et al., 1991) and used to improve the NCS and solvent flattening masks. A few iterations of this process led to an interpretable density for the entire p25⁶⁰. At early stages of model building, it also became clear that the activation loop of CDK5 had to be rebuilt. Model refinement was carried out with the CNS program suite (Brunger et al., 1998). After rigid body fitting, several runs of torsion angle molecular dynamics using strict NCS were applied, followed by positional and grouped B factor refinement, and manual model rebuilding. Toward the end of refinement, tight NCS restraints were introduced, and B factors were refined individually. All residues have ϕ - ψ angles falling within the most favored (84.5%) or additional allowed (15.5%) regions of the Ramachandran plot. Protein dissolved from CDK5-p25 crystals migrated indistinguishably from a fresh sample whose molecular weight had been verified by mass spectrometry, suggesting that the N- and C-terminal regions of p25 are present but disordered in the crystals. Threading analysis was carried out with the PSIPred 2.0 server (<http://insulin.brunel.ac.uk/psipred/>) (Jones, 1999).

CDK5 and GST-p20 Constructs

CDK5 point mutants S159A and S159E were generated by polymerase chain reaction (PCR) using complementary primers containing the mutation on a HA-tagged human CDK5 template. The PCR frag-

ments were subcloned into the BamHI site of pcDNA3 (Invitrogen) to create HA-CDK5^{S159A} and HA-CDK5^{S159E}. The CDK5^{S159T}, CDK5^{I153A}, and CDK5^{I153F} mutants were generated with the same strategy using human CDK5 as a template, and the resulting PCR product was subcloned into the EcoRV and BamHI site of pcDNA3. GST-p20 (aa 145–307 of human p35) was made by PCR on a GST-p35 (aa 1–307) template, and the PCR fragment was cloned into the EcoRI and SalI sites of PGEX-4T2 (Amersham-Pharmacia Biotech). The E240A and E240Q point mutants were generated using GST-p20 as a template. The PCR fragments were subcloned into the EcoRI and SalI sites of PGEX-4T2. All mutants were confirmed by sequencing.

Protein Purification of GST-p20 and CDK5

E. coli strain BL21(DE3) was transformed with expression vectors encoding GST-CDK5, GST-p20, GST-p20^{E240Q}, and GST-p20^{E240A}. Protein expression was induced with 0.2 mM IPTG for 4 hr at 37°C, and cells were harvested by centrifugation. The bacterial pellet was resuspended in 10 ml TNT buffer (50 mM Tris [pH 8.0], 200 mM NaCl, 2.5 mM EDTA, and 0.5% Tween-20) supplemented with protease inhibitor tablet (Roche Diagnostics). After sonication, 0.1% Triton X-100 was added, and the lysates were spun at 10,000 ×g for 30 min at 4°C. The lysate was absorbed to Glutathione Sepharose 4B (GSH, Amersham-Pharmacia), and the beads were washed three times with TNT buffer. Bound proteins were eluted with 15 mM Glutathione, 200 mM Tris (pH 8.0), and 0.1% Triton X-100, concentrated, and the buffer was exchanged to Buffer A (20 mM MOPS [pH 7.2] and 5 mM MgCl₂) using Millipore Ultrafree filters.

GST Pull-Down Assay

Purified GST, GST-p20, GST-p20^{E240Q}, or GST-p20^{E240A} in Buffer A were absorbed to GSH beads and crosslinked to the resin with 20 mM DMP (in 0.2 M Na Borate [pH 9.0]) for 1 hr at 4°C. The beads were washed with 0.2 M Ethanolamine [pH 8.0] and subsequently with E1A lysis buffer (50 mM Tris-HCl [pH 7.5], 250 mM NaCl, 5 mM EDTA [pH 8.0], and 0.1% Nonidet P-40). Cos7 cells transfected with CDK5 were lysed in E1A lysis buffer, and 500 µg of lysate was incubated with GSH beads crosslinked to 10 µg of GST fusion proteins. CDK5 binding to the different GST-fusion proteins was analyzed by Western blotting as previously described (Zukerberg et al., 2000).

In Vitro Kinase Assay

4 µg of GST-CDK5 and GST-p20 (or GST-p20^{E240Q} or GST-p20^{E240A}) were added to 500 µM peptide substrate in 30 µl Kinase Buffer (20 mM MOPS [pH 7.2], 5 mM MgCl₂, 1 mM DTT, 20 µM ATP, and 2.5 µCi [γ-32P] ATP [3000 Ci/mmol]). The reaction proceeded for 1 hr at room temperature. 100 µg of BSA was added, and the reaction was stopped by adding 30 µl of ice-cold 20% TCA. The samples were chilled for 5 min and spun for 2 min at 13K on a benchtop microcentrifuge. 20 µl of the supernatant was spotted on phosphocellulose disc papers (Gibco-BRL). The discs were washed four times for 10 min in 0.3% phosphoric acid, and the associated radioactivity was counted in 10 ml Safescint fluid. Peptide substrates were prepared by the Tufts Core Facility (Boston, MA).

Immunoprecipitation and Immunocomplex Kinase Assay

10 cm plates of Cos7 cells were transiently transfected using Lipofectamine2000 (Gibco-BRL) according to the manufacturer's instruction. 1 µg pcDNA3-p35 was cotransfected with 2 µg of pcDNA3-CDK5 or equivalent amounts of the CDK5^{S159A}, CDK5^{S159E}, CDK5^{S159T}, CDK5^{I153A}, or CDK5^{I153F} mutant vectors (see above). p35 immunoprecipitation and Western blot analysis of the CDK5-p35 complex from transfected lysates were carried out as previously described (Zukerberg et al., 2000). For kinase assays, p35 immunocomplexes bound to Protein A-Sepharose were washed three times with E1A lysis buffer and then two times with Buffer A. 30 µl of Kinase buffer containing 500 µM peptide substrate (PKTPAKAKKL) was incubated with the immunocomplex for 1 hr at room temperature. Samples were iced for 5 min and spun for 1 min in a benchtop microcentrifuge. 10 µl of the supernatant was spotted on Phosphocellulose disc paper and counted as described above.

Acknowledgments

We thank Lucia Massimiliano for technical support, Victor Lamzin and the staff of the EMBL-Hamburg outstation for help with data collection, Stephen C. Harrison, Kristian Helin, and Philip W. Hinds for critical reading of the manuscript, and Laurent Meijer, Neil McDonald, and David Owen for discussions. C.T. is supported through a grant of the International Association for Cancer Research (AICR) to A.M. A.M. is an EMBO Young Investigator and a Scholar of the Italian Foundation for Cancer Research (FIRC). The Structural Biology Unit at the European Institute of Oncology was created with the generous help of the Giovanni Armenise-Harvard Foundation for Advanced Medical Research.

Received March 21, 2001; revised July 26, 2001.

References

- Ahlijanian, M.K., Barrezaeta, N.X., Williams, R.D., Jakowski, A., Kowsz, K.P., McCarthy, S., Coskran, T., Carlo, A., Seymour, P.A., Burkhardt, J.E., et al. (2000). Hyperphosphorylated tau and neurofilament and cytoskeletal disruptions in mice overexpressing human p25, an activator of cdk5. *Proc. Natl. Acad. Sci. USA* 97, 2910–2915.
- Baumann, K., Mandelkow, E.M., Biernat, J., Pivnicka-Worms, H., and Mandelkow, E. (1993). Abnormal Alzheimer-like phosphorylation of tau-protein by cyclin-dependent kinases cdk2 and cdk5. *FEBS Lett.* 336, 417–424.
- Beaudette, K.N., Lew, J., and Wang, J.H. (1993). Substrate specificity characterization of a cdc2-like protein kinase purified from bovine brain. *J. Biol. Chem.* 268, 20825–20830.
- Bibb, J.A., Snyder, G.L., Nishi, A., Yan, Z., Meijer, L., Fienberg, A.A., Tsai, L.H., Kwon, Y.T., Girault, J.A., Czernik, A.J., et al. (1999). Phosphorylation of DARPP-32 by Cdk5 modulates dopamine signalling in neurons. *Nature* 402, 669–671.
- Bibb, J.A., Chen, J., Taylor, J.R., Svenningsson, P., Nishi, A., Snyder, G.L., Yan, Z., Sagawa, Z.K., Oulmet, C.C., Nairn, A.C., et al. (2001). Effects of chronic exposure to cocaine are regulated by the neuronal protein Cdk5. *Nature* 410, 376–380.
- Brown, N.R., Noble, M.E., Endicott, J.A., Garman, E.F., Wakatsuki, S., Mitchell, E., Rasmussen, B., Hunt, T., and Johnson, L.N. (1995). The crystal structure of cyclin A. *Structure* 3, 1235–1247.
- Brown, N.R., Noble, M.E., Endicott, J.A., and Johnson, L.N. (1999). The structural basis for specificity of substrate and recruitment peptides for cyclin-dependent kinases. *Nat. Cell Biol.* 1, 438–443.
- Brunger, A.T., Adams, P.D., Clore, G.M., DeLano, W.L., Gros, P., Grosse-Kunstleve, R.W., Jiang, J.S., Kuszewski, J., Nilges, M., Pannu, N.S., et al. (1998). Crystallography & NMR system: a new software suite for macromolecular structure determination. *Acta Crystallogr. D Biol. Crystallogr.* 54, 905–921.
- Canagarajah, B.J., Khokhlatchev, A., Cobb, M.H., and Goldsmith, E.J. (1997). Activation mechanism of the MAP kinase ERK2 by dual phosphorylation. *Cell* 90, 859–869.
- Card, G.L., Knowles, P., Laman, H., Jones, N., and McDonald, N.Q. (2000). Crystal structure of a gamma-herpesvirus cyclin-cdk complex. *EMBO J.* 19, 2877–2888.
- Carson, M. (1991). Ribbons 2.0. *J. Appl. Crystallography* 24, 958–961.
- Chae, T., Kwon, Y.T., Bronson, R., Dikkes, P., Li, E., and Tsai, L.H. (1997). Mice lacking p35, a neuronal specific activator of Cdk5, display cortical lamination defects, seizures, and adult lethality. *Neuron* 18, 29–42.
- Chin, K.T., Ohki, S.Y., Tang, D., Cheng, H.C., Wang, J.H., and Zhang, M. (1999). Identification and structure characterization of a Cdk inhibitory peptide derived from neuronal-specific Cdk5 activator. *J. Biol. Chem.* 274, 7120–7127.
- Chou, K.C., Watenpugh, K.D., and Heinrikson, R.L. (1999). A model of the complex between cyclin-dependent kinase 5 and the activation domain of neuronal Cdk5 activator. *Biochem. Biophys. Res. Commun.* 259, 420–428.
- CCP4 (Collaborative Computational Project 4) (1994). The CCP4

- suite: programs for protein crystallography. *Acta Crystallogr. D* 50, 760–763.
- De Bondt, H.L., Rosenblatt, J., Jancarik, J., Jones, H.D., Morgan, D.O., and Kim, S.H. (1993). Crystal structure of cyclin-dependent kinase 2. *Nature* 363, 595–602.
- Fletcher, A.I., Shuang, R., Giovannucci, D.R., Zhang, L., Bittner, M.A., and Stuenkel, E.L. (1999). Regulation of exocytosis by cyclin-dependent kinase 5 via phosphorylation of Munc18. *J. Biol. Chem.* 274, 4027–4035.
- Gibson, T.J., Thompson, J.D., Blocker, A., and Kouzarides, T. (1994). Evidence for a protein domain superfamily shared by the cyclins, TFIIB and RB/p107. *Nucleic Acids Res.* 22, 946–952.
- Hisanaga, S., Ishiguro, K., Uchida, T., Okumura, E., Okano, T., and Kishimoto, T. (1993). Tau protein kinase II has a similar characteristic to cdc2 kinase for phosphorylating neurofilament proteins. *J. Biol. Chem.* 268, 15056–15060.
- Ishiguro, K., Takamatsu, M., Tomizawa, K., Omori, A., Takahashi, M., Arioka, M., Uchida, T., and Imahori, K. (1992). Tau protein kinase I converts normal tau protein into A68-like component of paired helical filaments. *J. Biol. Chem.* 267, 10897–10901.
- Jeffrey, P.D., Russo, A.A., Polyak, K., Gibbs, E., Hurwitz, J., Massague, J., and Pavletich, N.P. (1995). Mechanism of CDK activation revealed by the structure of a cyclinA-CDK2 complex. *Nature* 376, 313–320.
- Jones, D.T. (1999). GenTHREADER: an efficient and reliable protein fold recognition method for genomic sequences. *J. Mol. Biol.* 287, 797–815.
- Jones, T.A., Zou, J.-Y., and Cowan, S.W. (1991). Improved methods for building protein models in electron density map and the location of errors in these models. *Acta Crystallogr. A* 47, 110–119.
- Ko, J., Humbert, S., Bronson, R.T., Takahashi, S., Kulkarni, A.B., Li, E., and Tsai, L.H. (2001). p35 and p39 are essential for cdk5 function during neurodevelopment. *J. Neurosci.* 21, 6758–6771.
- Kusakawa, G., Saito, T., Onuki, R., Ishiguro, K., Kishimoto, T., and Hisanaga, S. (2000). Calpain-dependent proteolytic cleavage of the p35 cyclin-dependent kinase 5 activator to p25. *J. Biol. Chem.* 275, 17166–17172.
- Kwon, Y.T., and Tsai, L.H. (1998). A novel disruption of cortical development in p35(-/-) mice distinct from reeler. *J. Comp. Neurol.* 395, 510–522.
- Lee, M.S., Kwon, Y.T., Li, M., Peng, J., Friedlander, R.M., and Tsai, L.H. (2000). Neurotoxicity induces cleavage of p35 to p25 by calpain. *Nature* 405, 360–364.
- Lew, J., Winkfein, R.J., Paudel, H.K., and Wang, J.H. (1992). Brain proline-directed protein kinase is a neurofilament kinase which displays high sequence homology to p34cdc2. *J. Biol. Chem.* 267, 25922–25926.
- Matsubara, M., Kusubata, M., Ishiguro, K., Uchida, T., Titani, K., and Taniguchi, H. (1996). Site-specific phosphorylation of synapsin I by mitogen-activated protein kinase and Cdk5 and its effects on physiological functions. *J. Biol. Chem.* 271, 21108–21113.
- Matsuoka, M., Matsuura, Y., Semba, K., and Nishimoto, I. (2000). Molecular cloning of a cyclin-like protein associated with cyclin-dependent kinase 3 (cdk 3) in vivo. *Biochem. Biophys. Res. Commun.* 273, 442–447.
- Miyajima, M., Nornes, H.O., and Neuman, T. (1995). Cyclin E is expressed in neurons and forms complexes with cdk5. *Neuroreport* 6, 1130–1132.
- Moffat, J., Huang, D., and Andrews, B. (2000). Functions of Pho85 cyclin-dependent kinases in budding yeast. *Prog. Cell Cycle Res.* 4, 97–106.
- Morgan, D.O. (1995). Principles of CDK regulation. *Nature* 374, 131–134.
- Nath, R., Davis, M., Probert, A.W., Kupina, N.C., Ren, X., Schielke, G.P., and Wang, K.K. (2000). Processing of cdk5 activator p35 to its truncated form (p25) by calpain in acutely injured neuronal cells. *Biochem. Biophys. Res. Commun.* 274, 16–21.
- Nguyen, M.D., Lariviere, R.C., and Julien, J.-P. (2001). Deregulation of cdk5 in a mouse model of ALS: toxicity alleviated by perikaryal neurofilament inclusions. *Neuron* 30, 135–147.
- Nicholls, A., Sharp, K.A., and Honig, B. (1991). Protein folding and association: insights from the interfacial and thermodynamic properties of hydrocarbons. *Proteins* 11, 281–296.
- Niethammer, M., Smith, D.S., Ayala, R., Peng, J., Ko, J., Lee, M.S., Morabito, M., and Tsai, L.H. (2000). NUDEL is a novel Cdk5 substrate that associates with LIS1 and cytoplasmic dynein. *Neuron* 28, 697–711.
- Noble, M.E., Endicott, J.A., Brown, N.R., and Johnson, L.N. (1997). The cyclin box fold: protein recognition in cell-cycle and transcription control. *Trends Biochem. Sci.* 22, 482–487.
- Ohshima, T., Ward, J.M., Huh, C.G., Longenecker, G., Veeranna, Pant, H.C., Brady, R.O., Martin, L.J., and Kulkarni, A.B. (1996). Targeted disruption of the cyclin-dependent kinase 5 gene results in abnormal corticogenesis, neuronal pathology and perinatal death. *Proc. Natl. Acad. Sci. USA* 93, 11173–11178.
- Otwinowski, Z. (1993). Oscillation Data Reduction Program., L. Sawyer, N. Isaacs, and S. Bailey, eds. (Warrington, UK: Science and Engineering Research Council/Daresbury Laboratory).
- Patrick, G.N., Zhou, P., Kwon, Y.T., Howley, P.M., and Tsai, L.H. (1998). p35, the neuronal-specific activator of cyclin-dependent kinase 5 (Cdk5) is degraded by the ubiquitin-proteasome pathway. *J. Biol. Chem.* 273, 24057–24064.
- Patrick, G.N., Zukerberg, L., Nikolic, M., de la Monte, S., Dikkes, P., and Tsai, L.H. (1999). Conversion of p35 to p25 deregulates Cdk5 activity and promotes neurodegeneration. *Nature* 402, 615–622.
- Paudel, H.K., Lew, J., Ali, Z., and Wang, J.H. (1993). Brain proline-directed protein kinase phosphorylates tau on sites that are abnormally phosphorylated in tau associated with Alzheimer's paired helical filaments. *J. Biol. Chem.* 268, 23512–23518.
- Poon, R.Y., Lew, J., and Hunter, T. (1997). Identification of functional domains in the neuronal Cdk5 activator protein. *J. Biol. Chem.* 272, 5703–5708.
- Qi, Z., Huang, Q.Q., Lee, K.Y., Lew, J., and Wang, J.H. (1995). Reconstitution of neuronal Cdc2-like kinase from bacteria-expressed Cdk5 and an active fragment of the brain-specific activator. Kinase activation in the absence of Cdk5 phosphorylation. *J. Biol. Chem.* 270, 10847–10854.
- Russo, A.A., Jeffrey, P.D., and Pavletich, N.P. (1996). Structural basis of cyclin-dependent kinase activation by phosphorylation. *Nat. Struct. Biol.* 3, 696–700.
- Schultz, J., Copley, R.R., Doerks, T., Ponting, C.P., and Bork, P. (2000). SMART: a web-based tool for the study of genetically mobile domains. *Nucleic Acids Res.* 28, 231–234.
- Sharma, P., Barchi, J.J., Jr., Huang, X., Amin, N.D., Jaffe, H., and Pant, H.C. (1998). Site-specific phosphorylation of Lys-Ser-Pro repeat peptides from neurofilament H by cyclin-dependent kinase 5: structural basis for substrate recognition. *Biochemistry* 37, 4759–4766.
- Sharma, P., Sharma, M., Amin, N.D., Albers, R.W., and Pant, H.C. (1999a). Regulation of cyclin-dependent kinase 5 catalytic activity by phosphorylation. *Proc. Natl. Acad. Sci. USA* 96, 11156–11160.
- Sharma, P., Steinbach, P.J., Sharma, M., Amin, N.D., Barchi, J.J., Jr., and Pant, H.C. (1999b). Identification of substrate binding site of cyclin-dependent kinase 5. *J. Biol. Chem.* 274, 9600–9606.
- Shuang, R., Zhang, L., Fletcher, A., Groblewski, G.E., Pevsner, J., and Stuenkel, E.L. (1998). Regulation of Munc-18/syntaxin 1A interaction by cyclin-dependent kinase 5 in nerve endings. *J. Biol. Chem.* 273, 4957–4966.
- Smith, D.S., Greer, P.L., and Tsai, L.H. (2001). Cdk5 on the brain. *Cell Growth Differ.* 12, 277–283.
- Solomon, M.J., and Kaldis, P. (1999). In *Results and Problems in Cell Differentiation*, M. Pagano, ed. (New York: Springer).
- Songyang, Z., Lu, K.P., Kwon, Y.T., Tsai, L.H., Filhol, O., Cochet, C., Brickey, D.A., Soderling, T.R., Bartleson, C., Graves, D.J., et al. (1996). A structural basis for substrate specificities of protein Ser/Thr kinases: primary sequence preference of casein kinases I and

II, NIMA, phosphorylase kinase, calmodulin-dependent kinase II, CDK5, and Erk1. *Mol. Cell. Biol.* **16**, 6486–6493.

Tang, D., Chun, A.C.S., Zhang, M., and Wang, J.H. (1997). Cyclin-dependent kinase 5 (Cdk5) activation domain of neuronal Cdk5 activator. Evidence of the existence of cyclin fold in neuronal Cdk5a activator. *J. Biol. Chem.* **272**, 12318–12327.

Xiong, Y., Zhang, H., and Beach, D. (1992). D type cyclins associate with multiple protein kinases and the DNA replication and repair factor PCNA. *Cell* **71**, 505–514.

Zukerberg, L.R., Patrick, G.N., Nikolic, M., Humbert, S., Wu, C.L., Lanier, L.M., Gertler, F.B., Vidal, M., Van Etten, R.A., and Tsai, L.H. (2000). Cables links Cdk5 and c-Abl and facilitates Cdk5 tyrosine phosphorylation, kinase upregulation, and neurite outgrowth. *Neuron* **26**, 633–646.

Accession Numbers

The coordinates of the CDK5-p25 complex have been deposited in the Protein Data Bank under ID code 1h41.